



An innovative design for cardiopulmonary resuscitation manikins based on a human-like thorax and embedded flow sensors

Proc IMechE Part H:
J Engineering in Medicine
2017, Vol. 231(3) 243–249
© IMechE 2017 
Reprints and permissions:
sagepub.co.uk/journalsPermissions.nav
DOI: 10.1177/0954411917691555
journals.sagepub.com/home/pih


Mark Thielen¹, Rohan Joshi^{1,2}, Frank Delbressine¹, Sidarto Bambang Oetomo^{1,3} and Loe Feijs¹

Abstract

Cardiopulmonary resuscitation manikins are used for training personnel in performing cardiopulmonary resuscitation. State-of-the-art cardiopulmonary resuscitation manikins are still anatomically and physiologically low-fidelity designs. The aim of this research was to design a manikin that offers high anatomical and physiological fidelity and has a cardiac and respiratory system along with integrated flow sensors to monitor cardiac output and air displacement in response to cardiopulmonary resuscitation. This manikin was designed in accordance with anatomical dimensions using a polyoxymethylene rib cage connected to a vertebral column from an anatomical female model. The respiratory system was composed of silicon-coated memory foam mimicking lungs, a polyvinylchloride bronchus and a latex trachea. The cardiovascular system was composed of two sets of latex tubing representing the pulmonary and aortic arteries which were connected to latex balloons mimicking the ventricles and lumped abdominal volumes, respectively. These balloons were filled with Life/form simulation blood and placed inside polyether foam. The respiratory and cardiovascular systems were equipped with flow sensors to gather data in response to chest compressions. Three non-medical professionals performed chest compressions on this manikin yielding data corresponding to force–displacement while the flow sensors provided feedback. The force–displacement tests on this manikin show a desirable nonlinear behaviour mimicking chest compressions during cardiopulmonary resuscitation in humans. In addition, the flow sensors provide valuable data on the internal effects of cardiopulmonary resuscitation. In conclusion, scientifically designed and anatomically high-fidelity designs of cardiopulmonary resuscitation manikins that embed flow sensors can improve physiological fidelity and provide useful feedback data.

Keywords

Cardiopulmonary resuscitation, chest compressions, medical simulation, medical training, feedback system, manikin

Date received: 21 April 2016; accepted: 10 January 2017

Introduction

Cardiopulmonary resuscitation (CPR) is an emergency procedure performed on patients during cardiac and respiratory arrest. This procedure externally activates the cardiac and respiratory systems via the delivery of chest compressions and artificial ventilation (e.g. rescue breathing). These actions aim at delivering oxygen to vital organs until spontaneous circulation and breathing can be restored.

Multiple organisations such as the American Health Association (AHA)¹ provide guidelines for performing CPR. For adults, these guidelines recommend a thoracic compression depth of 5 cm or more at the centre of the sternum at a rate of at least 100 compressions

per minute (CPM). These guidelines also recommend administering two rescue breaths (with a visible chest-rise) per 30 chest compressions. In order to train

¹Department of Industrial Design, Eindhoven University of Technology, Eindhoven, The Netherlands

²Department of Clinical Physics, Máxima Medisch Centrum Veldhoven, Veldhoven, The Netherlands

³Department of Neonatology, Máxima Medisch Centrum Veldhoven, Veldhoven, The Netherlands

Corresponding author:

Mark Thielen, Department of Industrial Design, Eindhoven University of Technology, Laplace 32, 5612 AZ Eindhoven, The Netherlands.
Email: m.w.h.thielen@tue.nl

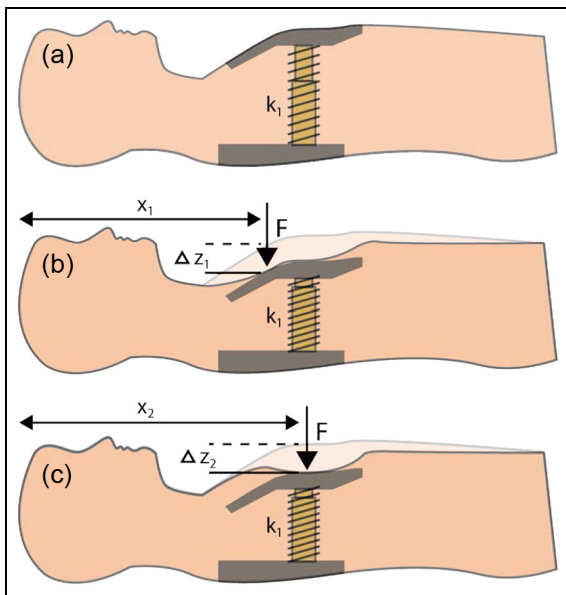


Figure 1. (a) An illustration of an uncompressed classical CPR manikin, (b) chest compression at a location left of centre and (c) chest compression at the centre of the thorax. In both examples of compression, $\Delta z_1 = \Delta z_2$ which is unrealistic when compared to the human body.

personnel in performing CPR, surrogate patients in the form of manikins are used.

Ideally, manikins should be designed based on an understanding of the physiological and mechanical effects of administering CPR with the aim of increasing realism during training so that clinical performance of CPR administration can be improved. Not surprisingly, the current fields of research in the design of CPR manikins include the following: theoretical foundations of simulation in healthcare,^{2,3} physiological modelling of the cardiovascular and respiratory systems,⁴⁻⁶ force-displacement testing of the human thorax,⁷⁻⁹ enhancing tactile experience of CPR manikins,¹⁰ effectiveness of using simulation in clinical practice¹¹⁻¹³ and incorporating clinical recommendations for manikin design.¹⁴

Despite the aforementioned recommendations and a clinical desire for physiologically and anatomically high-fidelity manikin designs, even the technologically most advanced manikins such as the SimMan 3G (Laerdal, Stavanger, Norway) and Apollo (CAE healthcare, Sarasota, FL, USA) do not fulfil all these requirements. This is partly due to the fact that like other classical designs, these manikins consist of a single spring-damper configuration, as illustrated in Figure 1(a), where the spring is represented by the diagonal stripes and the damper by the yellow cylinder. The behaviour of the spring with spring constant k_1 is that a vertical force F leads to a vertical displacement $\Delta z_1 = F/k_1$ (Figure 1(b)). This displacement is independent of the axial location (Figure 1(c)) of the applied force since the manikin sternum is stiff and does not tilt, a behaviour unrealistic when compared to the human body. Furthermore, while most classical manikins offer

depth detection and the rate of chest compression, thereby providing information on the adherence to CPR guidelines, they provide no feedback on the physiological and mechanical effects of performing CPR, for example, oxygen saturation and cardiac output.

There is a key clinical demand for CPR manikins to mimic human physiology and monitor cardiac output, artificial ventilation and oxygen saturation in order to provide feedback data for assessing CPR performance.^{15,16} This requires manikins to have an actual cardiovascular and respiratory system, within which necessary sensors can be embedded. In addition, manikins need an anatomically correct skeletal structure to increase tactile realism. A design that would incorporate these features will provide additional value over the existing designs since clinicians will be able to titrate their CPR actions in order to fulfil physiological demands.

This article details the design of such a manikin that incorporates an anatomically realistic thorax including a cardiovascular and respiratory system with integrated flow sensors for monitoring their output. Furthermore, we compare the force-displacement performance of our design to that of humans and classical manikin designs. Finally, we compare the cardiac output, as measured by the embedded sensors, to physiological and clinical studies.

Materials and methods

Modelling the thorax

In Figure 2(a), we show a theoretical improvement over a single spring-damper manikin configuration (Figure 1(a)). For the purpose of illustration, a configuration of

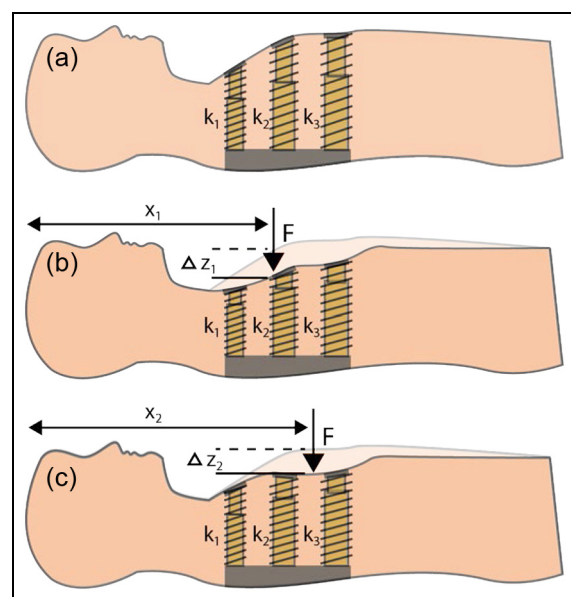


Figure 2. (a) A theoretical improvement over a single spring-damper configuration. (b and c) The same force at different locations will lead to different displacements, $\Delta z_1 \neq \Delta z_2$.

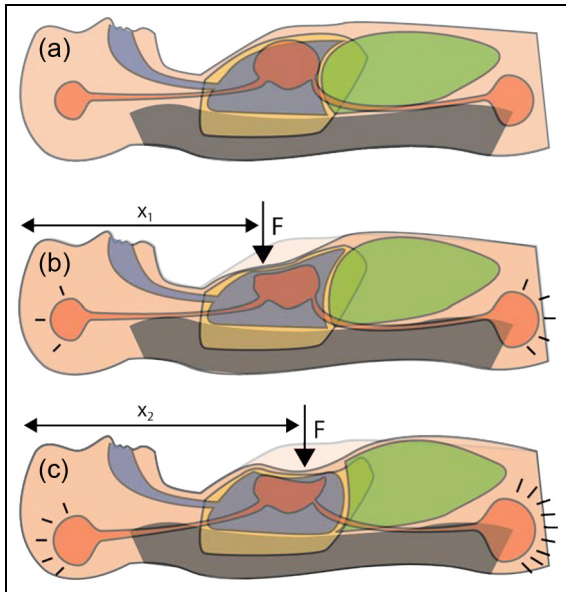


Figure 3. (a) Depiction of human anatomy. (b and c) Cardiac output is position-dependent (e.g. x_1 or x_2).

three spring–dampers is shown. A configuration of an infinite number of such spring–dampers would closely mimic the human thorax. In such a set-up, the spring behaviour of the thorax is dependent on the location of the force. The same force applied at different locations will lead to different displacements (Figure 2(b) and (c)), $\Delta z_1 \neq \Delta z_2$.

In Figure 3(a), we depict the human body in anatomical detail consisting of a flexible sternum/rib cage along with a respiratory and cardiovascular system. Grey depicts the spinal column to which the rib cage (yellow) is attached. The respiratory (blue) and cardiovascular (red) systems are present within the rib cage. The blood vessels in the cardiovascular system are lumped into cranial and abdominal blood volumes (shown as two red circles at the far ends of the body). The green area depicts the abdomen. Figure 3(b) and (c) depicts the internal effects occurring as a result of chest compressions. The effects of compression are position-dependent (clearly visible) and also modulate cardiac output.¹⁷

The manikin constructed for this research (Figure 4) was designed by combining the models as shown in Figures 2 and 3. Here, the rib cage, respiratory and cardiovascular systems mimic a configuration of multiple spring–damper systems. The next section details the design of this manikin.

Design of the new manikin and integration of sensors

As a foundation for the manikin design, a vertebral column (78 cm in height from pelvis to C1 vertebra) from an anatomical female model (vertebral column for the demonstration of malpositions; Erler-Zimmer, Lauf, Germany) was used. The rib cage of this model was

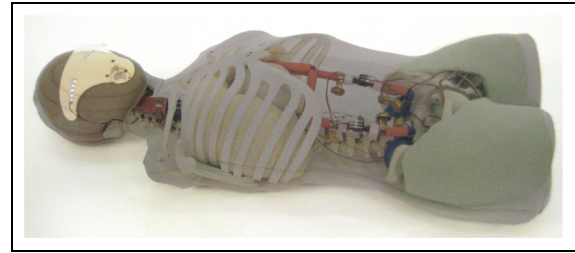


Figure 4. See-through image of a novel manikin design with human-like internal construction.

removed and copied on a 1:1 scale using the software Illustrator (Adobe, San Jose, CA, USA). This drawing was cut using a Speedy 300 laser engraver (Trotec, Canton, MI, USA) from a sheet of polyoxymethylene (POM) material (dimensions: 700 mm \times 400 mm \times 4 mm). The rib cage was bent into an anatomically correct shape using heat (Figure 5(a)) and the original reference model removed from the vertebral column. This rib cage was then socketed and bolted to the T1–T10 vertebrae of the skeletal model's spine (Figure 5(b)). The motivation for choosing POM was the expectation of forceful compressions,¹⁸ and it was chosen for its high stiffness property. In addition, POM has a high abrasion resistance and resilience to repeated load¹⁹ which are necessary material qualities for a model subjected to sustained compressions.

A respiratory system (lungs, bronchus and trachea) was created and embedded within this rib cage. The lungs were built using polyurethane (PU) memory foam (density, $\rho = 45 \text{ kg/m}^3$). This material was chosen to mimic the porous structure of lung tissue.^{20–22} Two foam blocks were carved into the anatomic shape (Figure 6) of lungs and coated with a layer of Ecoflex 00-30 silicon (Smooth-On, Macungie, PA, USA) to create closed chambers. These chambers were attached to bronchi made of polyvinylchloride (PVC), which in turn were connected to a trachea made of a latex tube (inner diameter, 2 cm). This trachea ended in the oral cavity of the manikin.

In addition to the respiratory system, a cardiovascular system was constructed and embedded within this rib cage. The system contained two sets of latex tubing (inner diameter, 1 cm) representing the pulmonary and aortic arteries. The four ends of these tubes were connected to latex balloons (Figure 6), two mimicking ventricles and two mimicking lumped abdominal blood volumes. All balloons were filled with 75 mL of Life/form simulation blood (Nasco, Fort Atkinson, WI, USA). This volume correlates with the average blood volume present in the ventricles of the female human body.²³ Both ventricles were inserted into a two-pocketed single polyether (PE) foam (density, $\rho = 25 \text{ kg/m}^3$) model representing the heart walls (Figure 7(a)). The heart model was placed inside the thorax, between the fourth and seventh rib, along the coronal cardiac axis of 45° slightly left of the sternum.

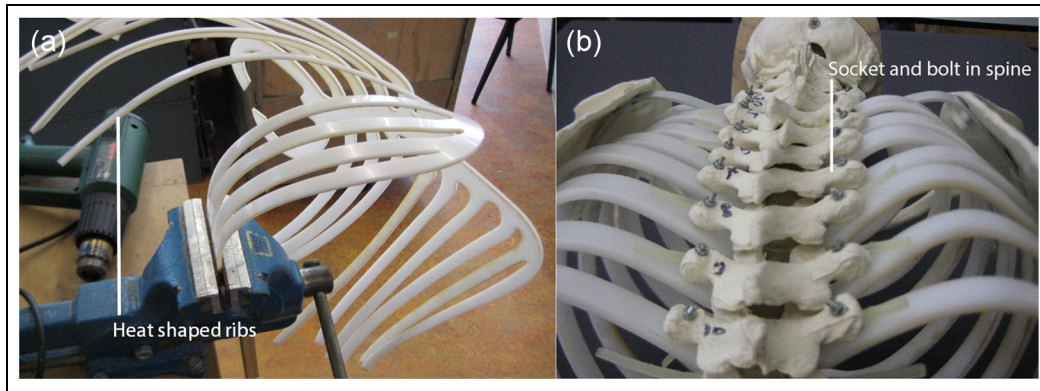


Figure 5. (a) An anatomically correct rib cage cut from 4-mm-thick POM material being bent into shape. (b) The rib cage socketed in and bolted to the spine.

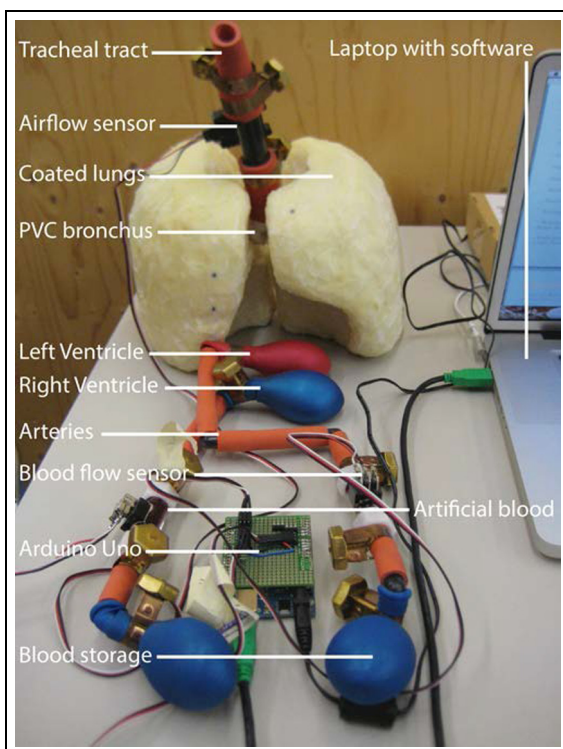


Figure 6. The set of artificial organs and body parts present in the manikin. From top to bottom: tracheal tract, airflow sensor, lungs, bronchi, left and right ventricles, pulmonary and aortic arteries, liquid flow turbine sensors, Arduino Uno microcontroller connected to laptop and lumped abdominal blood volumes.

The respiratory and cardiovascular systems were equipped with flow sensors to gather data in response to chest compressions. An AMW720P1 airflow sensor (Honeywell, Morris Plains, NJ, USA) was embedded into the trachea. Two Vision 2000 flow sensors (B.I.O-TECH, Vilshofen, Germany) were embedded in the aortic and pulmonary arteries (Figure 6). An Arduino Uno microprocessor platform was used (ARDUINO LLC, Somerville, MA, USA) for collecting and processing the data from sensors. These data were displayed on

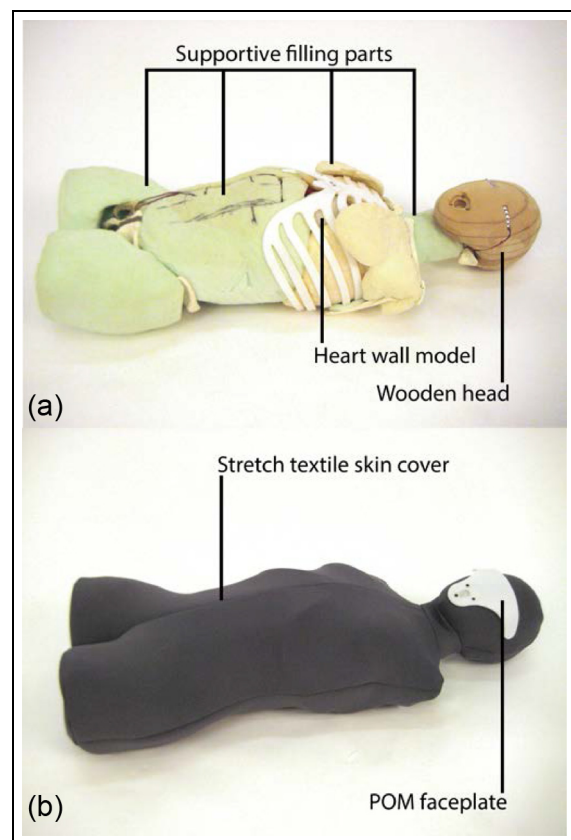


Figure 7. (a) The manikin with head, abdomen and muscle padding. (b) Outer skin cover and faceplate.

a laptop (Figure 6) in real-time using Processing software (Creative Commons, Mountain View, CA, USA).

The manikin was completed by incorporating a wooden head and foam-based musculature for the neck, shoulders, abdominal wall and thighs, respectively. The abdominal musculature was created to secure the thoracic organs (Figure 7(a)) while the other body parts were created to improve the aesthetics of the manikin. Finally, a stretch-textile cover (skin) and POM faceplate were created to secure all parts of the manikin in place (Figure 7(b)).

Test set-up

In order to estimate the mechanical behaviour of the thorax, force–displacement tests were performed on the CPR manikin using the Q-CPR measurement and feedback tool (Philips, Eindhoven, The Netherlands). Three non-medical professionals performed a series of 30-s long chest compressions on the manikin. These compressions were performed in conformance with the AHA guidelines for speed and compression depth. The force of compressions in Newton and the depth of thoracic displacement (in cm) were measured with respect to time and were analysed using MATLAB (MathWorks, Natick, MA, USA). For one of the force–displacement tests, cardiac output and ventilation volume were captured using the embedded sensors. These sensors measured air displacement and ventricular blood flow. These sensor data were captured using the Arduino microcontroller and displayed using Processing.

Comparing force–displacement data with existing research

The results of the force–displacement tests, as obtained in our test set-up, were compared with the results of thoracic displacement research on typical humans and typical classical CPR manikins as reported by Gruben and colleagues.^{7–9} In their study, Gruben et al. fit a polynomial equation to their data as follows

$$F = F_e + F_d \quad (1)$$

$$F_e = k(z) \cdot z \quad (2)$$

$$k(z) = k_1 + k_2 \cdot z + k_3 \cdot z^2 + k_4 \cdot z^3 \quad (3)$$

$$F_d = \mu(z) \cdot \dot{z} \quad (4)$$

$$\mu(z) = d_0 + d_1 \cdot z \quad (5)$$

where the compression force F consists of an elastic component, F_e , and a damping component, F_d (equation (1)). The elastic component (F_e) is nonlinear since the stiffness coefficient, $k(z)$, is dependent on displacement (equations (2) and (3)). The damping component (F_d) depends on the damping coefficient $\mu(z)$ (equations (4) and (5)) which is also dependent on displacement.

Gruben et al. estimated $k(z)$ and $\mu(z)$ by fitting them to polynomials of four and two coefficients, respectively, as shown in equation (6)

$$F = k_1 \cdot z + k_2 \cdot z^2 + k_3 \cdot z^3 + k_4 \cdot z^4 + d_0 \dot{z} + d_1 \cdot z \cdot \dot{z} \quad (6)$$

The results of the compression force and the resulting vertical displacement (depth), as obtained from our tests, were fit to the above equation using the linear least squares method.

Comparing flow sensor data with existing research

We report the average cardiac output and air displacement (L/min) as measured by flow sensors in response

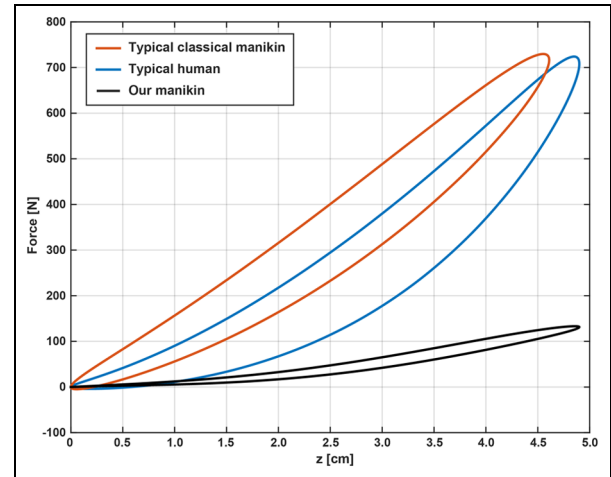


Figure 8. The force–displacement graphs for a typical classical manikin (red), the typical human (blue) and the manikin designed in this research (black). As the compression depth approaches 5 cm (as required by the AHA guidelines), our manikin shows a desirable nonlinear behaviour mimicking that seen in humans.

to chest compressions. These data are compared to the physiological model of Koeken et al.⁶ which was developed to investigate the cardiac output during CPR. Since the ventricular volumes of the manikin developed in this research (150 mL) and those of Koeken et al. (262 mL) are different, we proportionally scale the cardiac output obtained. Furthermore, the results of cardiac output are also compared with those of Fodden et al.²⁴ who estimated the cardiac output using Doppler ultrasound during CPR in humans.

Results

Comparing results of force–displacement

Figure 8 shows the force–displacement graphs for the typical classical manikins (red), typical humans (blue) as well as the manikin designed in this research (black). Each curve consists of the elastic component (compression) and the damping component (release). The areas under the curve correspond to the energy transmitted into the manikin/body during chest compressions (the work (W)). As the compression depth approaches 5 cm (as required by the AHA guidelines), our manikin shows a desirable nonlinear behaviour mimicking that of humans (blue). However, the force required to reach similar compression depths is considerably lower.

Comparing results obtained from sensor data

Figure 9 shows the cardiac output of the left (blue) and right (green) ventricle as well as the air displacement volume (red) during 18 consecutive chest compressions performed at 120 CPM in conformance with the AHA guidelines. The total cardiac output was found to be 1.65 L/min, 0.92 L/min in the left ventricle and 0.73 L/min in the right ventricle. As opposed to the model of

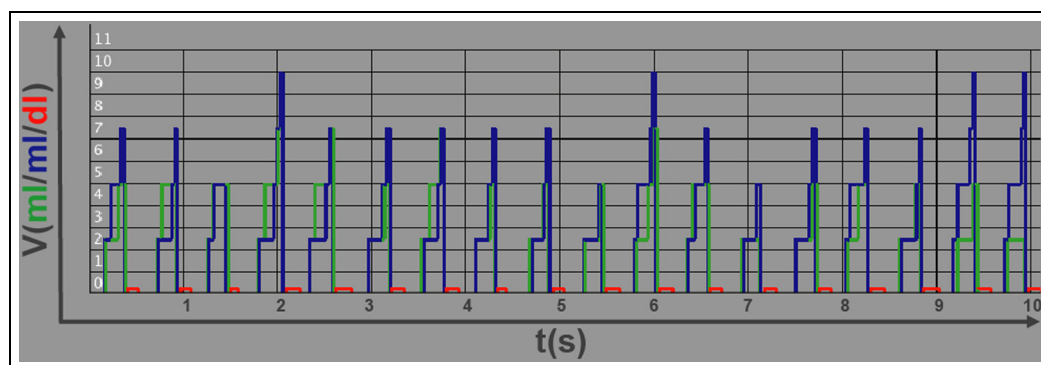


Figure 9. The cardiac output of the left (blue) and right (green) ventricle along with the air displacement volume (red) during 18 consecutive chest compressions performed at 120 compressions per minute (CPM) in conformance with the AHA guidelines.

Koeken et al.,⁶ we found a 43% higher cardiac output in our manikin. After scaling the cardiac output based on ventricular size, the cardiac output increased to 2.88 L/min, which is 150% higher. The cardiac output of 1.65 L/min in our manikin is 48% lower than that estimated by Fodden et al.²⁴ in human beings. Furthermore, the air displacement as measured in the trachea of our manikin during chest compressions was 2.7 L/min.

Discussion

This article details the design of a novel CPR manikin that anatomically mimics human beings. This human-like construction allows for the embodiment of vital organs within which flow sensors are integrated in order to measure cardiac output and air displacement. The novelty of this design is the anatomical design and construction of the manikin with the expectation that improving physical fidelity increases functional fidelity as showcased by Sawyer et al.¹³ in training simulators for intubation. The embodiment of flow sensors within the organs permits internal monitoring during CPR performance for which there is a strong clinical need.¹⁴ This biofeedback is expected to enhance understanding of the internal effects of performing CPR in terms of adequacy of ventilation and blood flow.

The force–displacement tests carried out to understand the mechanical behaviour of the thorax show that as the compression depth approaches 5 cm (as required by the AHA guidelines), the manikin designed in our research exhibits a desirable nonlinear behaviour as seen in humans. Our manikin, unlike typical manikins, shows a greater nonlinear relationship since the polynomial estimate of the force–displacement relationship (equation (6)) has three non-zero higher order components (k_2 , k_3 and k_4) while the typical manikin has only one higher order component (k_2).⁹

However, the force required to achieve similar compression depths in humans is considerably higher.⁹ This indicates that the stiffness of our manikin is low. The stiffness can be improved using an alternative material for the rib cage (e.g. fibreglass-coated ribs), increasing

the thickness of the rib cage and/or using a foam of higher density for lungs. Developing a thicker rib cage was restricted by our manufacturing constraints (Speedy 300 laser engraver) while higher density foams mimicking the density of lung tissue²⁵ are unavailable. The energy transmitted into the manikin (the work (W)) can be increased by enhancing the damping coefficient of the thorax which can be facilitated by connecting the lungs to the rib cage, that is, mimicking the pleural cavity and implementing flow restrictions. This, in addition to an increased stiffness, will mimic the force–displacement behaviour of human thorax more closely.

The flow sensors measuring cardiac output and air displacement during CPR provide useful data since the CPR trainee can immediately view the effects of their actions. The cardiac output data generated here are 48% lower than that measured by Fodden et al.²⁴ while being 150% higher than expected from physiological modelling.⁶ Likely, our results differ from those of Fodden et al. since their population was 70% male with potentially higher ventricular volumes, than our modelled subject who was female. In addition, less energy was transmitted into the thorax of the manikin during chest compressions, as can be seen from the force–displacement curves in Figure 8. The cardiac output of this manikin can be increased using larger latex balloons to mimic the ventricles and using latex tubing of a greater diameter to represent the pulmonary and aortic arteries. However, there is a need for conclusive clinical data on the cardiac output of humans during CPR before models can simulate physiologically realistic cardiac outputs.

This design also has some limitations. For example, it can be improved by employing materials that mimic the mechanical properties of human tissues more closely. The challenge herein is that the materials not only need to have suitable material properties but should also be amiable to the rigours of manufacturing processes such as laser cutting, heat shaping and injection moulding. The design is also limited by the absence of valves and the lack of connection between pulmonary and systemic circulations. These limitations

notwithstanding, this design makes important steps towards making the design of manikins more realistic and in improving anatomical and physiological fidelity.

Conclusion

This study details a scientifically designed novel manikin design that integrates cardiac and respiratory systems and offers increased anatomical and physiological fidelity. In response to CPR, this manikin shows a desirable nonlinear behaviour in its force–displacement curve, as is also seen in human beings. Furthermore, internal flow sensors monitoring cardiac output and air displacement provide valuable feedback.

Acknowledgements

This research was performed within the framework of IMPULS perinatology.

Declaration of conflicting interests

The author(s) declared no potential conflicts of interest with respect to the research, authorship and/or publication of this article.

Funding

The author(s) received no financial support for the research, authorship and/or publication of this article.

References

1. Neumar RW, Otto CW, Link MS, et al. Part 8: adult advanced cardiovascular life support: 2010 American Heart Association Guidelines for Cardiopulmonary Resuscitation and Emergency Cardiovascular Care. *Circulation* 2010; 122(18 Suppl. 3): S729–S767.
2. Dieckmann P, Gaba D and Rall M. Deepening the theoretical foundations of patient simulation as social practice. *Simul Healthc* 2007; 2(3): 183–193.
3. Zigmont JJ, Kappus LJ and Sudikoff SN. Theoretical foundations of learning through simulation. *Semin Perinatol* 2011; 35(2): 47–51.
4. Van Meurs WL, Good ML and Lampotang S. Functional anatomy of full-scale patient simulators. *J Clin Monit* 1997; 13: 317–324.
5. Couto CS. Mathematical models for educational simulation of cardiovascular pathophysiology, 2009, <https://repositorio-aberto.up.pt/bitstream/10216/60409/1/000137145.pdf>
6. Koeken Y, Aelen P, Noordergraaf GJ, et al. The influence of nonlinear intra-thoracic vascular behaviour and compression characteristics on cardiac output during CPR. *Resuscitation* 2011; 82(5): 538–544.
7. Bankman IN, Gruben KG, Halperin HR, et al. Identification of dynamic mechanical parameters of the human chest during manual cardiopulmonary resuscitation. *IEEE Trans Biomed Eng* 1990; 37(2): 211–217.
8. Gruben KG, Romlein J, Halperin HR, et al. System for mechanical measurements during cardiopulmonary resuscitation in humans. *IEEE Trans Biomed Eng* 1990; 37(2): 204–210.
9. Gruben KG, Halperin HR, Popel AS, et al. Sternal force-displacement relationship during cardiopulmonary resuscitation. *IEEE Trans Biomed Eng* 1999; 46(7): 788–796.
10. Stanley AA, Healey SK, Maltese MR, et al. Recreating the feel of the human chest in a CPR manikin via programmable pneumatic damping. In: *Proceedings, IEEE Haptics Symposium*, March 2012, pp.37–44. doi: 10.1109/HAPTIC.2012.618376710.1109/HAPTIC.2012.6183767
11. Martin PS, Kemp AM, Theobald PS, et al. Do chest compressions during simulated infant CPR comply with international recommendations? *Arch Dis Child* 2013; 98(8): 576–581.
12. Sawyer T, Sierocka-Castaneda A, Chan D, et al. Deliberate practice using simulation improves neonatal resuscitation performance. *Simul Healthc* 2011; 6(6): 327–336.
13. Sawyer T, Strandjord TP, Johnson K, et al. Neonatal airway simulators, how good are they? A comparative study of physical and functional fidelity. *J Perinatol* 2016; 36(2): 151–156.
14. Maconochie I and Bingham R. How to perform cardiopulmonary resuscitation: an opportunity for technology development. *Arch Dis Child* 2013; 98(8): 571–572.
15. Martin PS, Kemp AM, Theobald PS, et al. Does a more ‘physiological’ infant manikin design effect chest compression quality and create a potential for thoracic over-compression during simulated infant CPR? *Resuscitation* 2013; 84(5): 666–671.
16. Hamstra SJ, Brydges R, Hatala R, et al. Reconsidering fidelity in simulation-based training. *Acad Med* 2014; 89(3): 387–392.
17. Qvigstad E, Kramer-Johansen J, TømteØ, et al. Clinical pilot study of different hand positions during manual chest compressions monitored with capnography. *Resuscitation* 2013; 84(9): 1203–1207.
18. Tomlinson AE, Nysaether J, Kramer-Johansen J, et al. Compression force–depth relationship during out-of-hospital cardiopulmonary resuscitation. *Resuscitation* 2007; 72(3): 364–370.
19. Ashby MF. *Materials selection in mechanical design*. Amsterdam: Butterworth-Heinemann, 2005, p.624.
20. Maksym GN and Bates JHT. A distributed nonlinear model of lung tissue elasticity. *J Appl Physiol* 1997; 82(1): 32–41.
21. Kang SM, Lee SJ and Kim BK. Shape memory polyurethane foams. *Express Polym Lett* 2012; 6(1): 63–69.
22. Herman IP. *Physics of the Human Body*. Berlin: Heidelberg Springer-Verlag, 2007, doi: 10.1007/978-3-540-29604-1
23. Clay S, Alfakih K, Radjenovic A, et al. Normal range of human left ventricular volumes and mass using steady state free precession MRI in the radial long axis orientation. *MAGMA* 2006; 19(1): 41–45.
24. Fodden DI, Crosby AC and Channer KS. Doppler measurement of cardiac output during cardiopulmonary resuscitation. *J Accid Emerg Med* 1996; 13: 379–382.
25. Nebuya S, Koike T, Imai H, et al. Feasibility of using ‘lung density’ values estimated from EIT images for clinical diagnosis of lung abnormalities in mechanically ventilated ICU patients. *Physiol Meas* 2015; 36: 1261–1271.